nature communications

Article

https://doi.org/10.1038/s41467-025-67659-8

Mechanism of alternative splicing of yeast *HEH1* through competing 5′ splice sites

Received: 7 July 2025

Accepted: 5 December 2025

Published online: 16 December 2025

Check for updates

Ankita Katoch Banyal[1], Poulami Choudhuri[1], Balashankar R. Pillai[1,2], Amjadudheen Varikkapulakkal[1] & Shravan Kumar Mishra[1]

Alternative splicing of precursor-messenger RNAs (pre-mRNA) bearing introns with competing 5′ splice sites (5′SS) produces two mRNAs. We investigated the mechanism of alternative splicing of the yeast *HEH1/SRC1* gene, which contains four nucleotide-apart competing 5′SS, by monitoring its RNA and protein products. *HEH1* alternative splicing requires a sixteen-nucleotide pre-mRNA segment spanning its two 5′SS. The nucleotides are decoded by U5 and U6 small nuclear RNAs (snRNAs), supported by specific proteins of the spliceosomal B and Bact complexes, including Prp8. *HEH1* alternative splicing became independent of the supporting proteins following recalibration of the pre-mRNA-snRNA base pairings through changes in the 5′SS or U5 and U6 snRNAs. Assisted by proteins that stabilize low-fidelity, high-efficiency spliceosome conformations, the competing *HEH1* 5′SS are marked for alternative splicing by U5 and U6 snRNAs during the B to Bact transition of the spliceosome.

Splicing of precursor-messenger RNAs (pre-mRNA) occurs through a multi-step process involving large and dynamic ribonucleoprotein (RNP) complexes called spliceosomes. Stage-specific spliceosomes are assembled on a pre-mRNA following intricate rearrangements of five distinct snRNPs containing cognate small nuclear RNAs (snRNAs) and associated proteins[1,2]. Specific trans-acting snRNPs recognise cis-acting splicing signals in pre-mRNAs: the donor 5′ splice site (5′SS) 'GU', the acceptor 3′ splice site (3′SS) 'AG', and the branchpoint adenosine 'A'. Two steps of transesterification reactions, catalysed by divalent metal ions and U6 snRNA in the spliceosomes, remove introns and join exons to form functional mRNA. The spliceosome machinery is essential for constitutive and alternative splicing.

Multiple mRNAs can be produced from the same gene through alternative splicing. The process amplifies protein diversity from limited gene pools in an organism[3,4]. Different classes of alternative splicing exist in eukaryotes. Key among them occurs through the alternative selection of competing 5′SS[5] and 3′SS[4], and alternative splicing through competing 5′SS is a prevalent mode. A majority of pre-mRNAs in the budding yeast *Saccharomyces cerevisiae* have the highly conserved GUAUGU hexanucleotide as 5′SS donors[6], but the sequences are highly variable in intron-rich eukaryotes, where alternative 5′SS selection is widespread[7]. Two major classes of 5′SS (NN/GURAG and AG/GUNNN; N represents any nucleotide and R represents a purine, '/' indicates exon-intron junction), distinguished by the presence of 'G' at −1 and +5 positions, have been reported[8]. Alternative 5′SS are often found 4 nucleotides across the dominant 5′SS, and such occurrences in the human genome are estimated to be large[9,10]. The canonical 'GU' dinucleotide deviates to 'GC' in 0.87% of 5′SS in humans[11].

The *HEH1* gene (also called *SRC1*) in *S. cerevisiae* is alternatively spliced[12–14]. Its pre-mRNA has alternative donors with 'GC' and 'GU' dinucleotides embedded into two non-canonical 5′SS, /GCAAGU and /GUGAGU, arranged as a partially overlapping sequence /GCAA/GUGAGU. /GUGAGU is the dominant 5′SS, and splicing through this site generates mRNA-encoding a longer full-length protein, Heh1L. Splicing through the upstream /GCAAGU is tightly regulated and produces mRNA-encoding a shorter protein, Heh1S (the removal of the GCAA tetranucleotide gains an in-frame stop codon early in *HEH1S* mRNA). The two proteins share a common N-terminus but differ in their C-termini, thus attaining different topologies within the inner nuclear membrane and having distinct functions[15–18].

Competing 5′SS are selected through early recognition of pre-mRNAs by RBPs (RNA-binding proteins), U1 snRNA and associated

[1]Department of Biological Sciences, Indian Institute of Science Education and Research (IISER) Mohali, Mohali, India. [2]Present address: Institute of Molecular Biotechnology of the Austrian Academy of Sciences (IMBA), Vienna BioCenter (VBC), Dr Bohr-Gasse 3, 1030 Vienna, Vienna, Austria.
e-mail: skmishra@iisermohali.ac.in

proteins[19–21]. Specific RBPs, SR (serine/arginine-rich) proteins, and hnRNPs (heterogeneous nuclear ribonucleoproteins) have been reported to be crucial for 5′SS selection[5,22–27]. These proteins act as splicing enhancers and silencers, and regulate spliceosome assembly on target pre-mRNAs in association with the U1 snRNP. The yeast *RPL22B* gene possesses an alternative 5 ′ splice site (5′SS) decoded through U1 snRNP-associated proteins, including Nam8 and Mud1[28]. β globin, MAPT, and WT1 genes in humans utilise the core U1 snRNP proteins (U1-70K, U1A, U1C) and regulatory splicing factors such as SR proteins and hnRNPs to modulate alternative 5′SS choice[29].

The role of successive spliceosomal complexes in 5′SS selection has been reported[30]. U5 and U6 snRNAs modulate 5′SS selection[8,31]. In the absence of an authentic 5′SS, U5 snRNA can promote splicing from cryptic sites[32,33]. U1 snRNA-induced selection of a nearby 5′SS by U6 snRNA during spliceosome assembly[34]. m6A modification (methyl group addition at N6 position of adenosine) of U6 snRNA in humans, *Caenorhabditis elegans*, and *Schizosaccharomyces pombe* altered 5′SS selection, particularly of +4A positions in introns, and caused a shift to an alternative nearby site[35,36]. Furthermore, RNA structures modulate cis motifs in pre-mRNAs at different stages of the splicing cycle. A large number of *S. cerevisiae* introns are structured[37]. Structured introns in fission yeast and human are also regulatory to splicing outcomes and alternative splicing[38,39]. Thus, 5′SS selection depends on both early recognition and late processing of target introns.

The *HEH1* gene is a valuable tool for investigating the RNA and protein factors required for alternative splicing through competing and overlapping 5′ SS. Its alternative splicing requires non-covalent associations of the ubiquitin-like protein Hub1 (UBL5 in humans) with the U1 and U2 snRNP-bridging RNA helicase Prp5[40], and the U4/U6.U5 tri-snRNP protein Snu66[13]. Thus, Hub1 acts early in spliceosome assembly by activating the RNA helicase, as well as later with the tri-snRNP component[41]. The latter activity suggests a possible role of the spliceosome core in *HEH1* 5′SS selection. We find that *HEH1* alternative splicing requires optimal pairing of U5 and U6 snRNAs across a 16-nucleotide segment of the pre-mRNA across the two 5′SS at the exon1-intron boundary. The selection of the competing 5′SS by U5 and U6 snRNAs and alternative splicing was supported by specific proteins of the spliceosome core, including Prp8.

Results

Trans-acting proteins for *HEH1* alternative splicing

Between two 5′SS of *HEH1/SRC1* pre-mRNA/GCAA/GUGAGU, the usage of the upstream 5′SS/GCAAGU requires non-covalent binding of the ubiquitin-like protein Hub1 to Snu66. The downstream 5′SS/GUGAGU was dominant and selected independently of this complex[13]. We searched for additional *HEH1* alternative splicing factors in *S. cerevisiae* through the following approaches.

(i) *HEH1–LACZ* alternative splicing reporters *HEH1S–LACZ* and *HEH1L–LACZ* were prepared (Supplementary Fig. 1a), on the line of *RP51–LACZ* splicing reporter[42], by fusing a *HEH1* gene segment containing parts of the exons across the intron upstream of the β-galactosidase-encoding *LACZ* gene. In-frame translatable reporter mRNA would be made only after precise 5′SS selection and excision of the intron. Reporter activities were monitored in yeast strains grown on solid (X-Gal overlay assay) and liquid (ONPG assay) media. Splicing from the alternative 5′SS was diminished in the deletion strains of the RES (Retention and Splicing complex) complex subunits Snu17, Bud13, Pml1, and Urn1. The deletion of the NTC (Nineteen Complex) factor Ecm2 showed similar defects (Supplementary Fig. 1b, c). By contrast, splicing from the dominant 5′SS remained unaltered in the mutants, suggesting a role of these proteins in the selection of the weaker alternative 5′SS.

(ii) Heh1 protein isoforms were monitored in deletion and point mutants of splicing factors by Western blot assays. The gene was expressed with N-terminal epitope tags from a plasmid or tagged chromosomally. Supporting the data with the reporter assays (Supplementary Fig. 1a–c), Heh1S protein was strongly diminished in the knockout mutants of Snu17, Bud13, Pml1, and Urn1, in addition to Hub1 (Supplementary Fig. 1d). The previously reported D22A and H63L mutants of Hub1 were defective in *HEH1* alternative splicing. Potential RNA-binding mutant of Hub1, as deduced from cryo-EM studies of spliceosomes[43,44], showed a similar lack of Heh1S protein (Supplementary Fig. 1h). Alternative splicing defect was also seen in the Hub1-binding-deficient Snu66-HIND mutant (Supplementary Fig. 1j). Prp8 alleles were also screened for *HEH1* alternative splicing. Heh1S level was strongly reduced in the *prp8-101* (E1960K) allele. No other Prp8 mutant tested showed similar defects. While Heh1S protein was diminished in the above mutants, they showed more Heh1L than wt (Fig. 1a), possibly because the lack of competition from *HEH1S* 5′SS led to increased usage of the *HEH1L* site.

(iii) *HEH1* mRNA isoforms in the yeast mutants were monitored by reverse-transcription (RT) PCR assays, with primers binding to *HEH1* exons, followed by sequencing of the cDNAs. The two mRNAs show a single band. Since they differ in GCAA nucleotides at the exon junction (*HEHL* gains GCAA due to the usage of downstream 5′SS), electropherograms show two mixed peaks after the common exon. Areas under the peaks were integrated to estimate the relative abundance of the two mRNAs. Consistent with the findings from reporter assays and protein analysis, the above mutants showed diminished levels of *HEH1S* mRNA, confirming the 5′SS selection defects at the RNA level (Fig. 1c). The electropherograms also showed increased *HEH1L* mRNA level in the mutants, compared to the wt strain (Fig. 1d), consistent with higher protein levels seen in Fig. 1a. Thus, spliceosomes defective in using *HEH1S* 5′SS used the dominant *HEH1L* 5′SS more efficiently in the absence of competition.

(iv) Splicing factors essential for cell viability could not be explored with deletion strains. Hub1's proximity to them was used to explore their potential role in *HEH1* alternative splicing. Snu66-binding-deficient *hub1*(*D22A*) in the free form was defective in the usage of *HEH1* alternative 5′SS, but its linear fusion to Snu66, Prp38 and Prp8 restored alternative splicing in cells lacking Hub1[13]. Interestingly, Heh1S protein was restored after anchoring Hub1 to Prp3, Prp6, and Prp31, but not to other proteins or the components of U1 and U2 snRNPs (Fig. 1e). Thus, Hub1's proximity to specific proteins of the spliceosome B and Bact complexes (Snu66, Prp38, Prp8, Prp3, Prp6, and Prp31) promoted *HEH1* alternative splicing.

The data discussed in i-iv indicated the need for specific proteins of the spliceosome core for *HEH1S* formation. However, their excess did not dominate the 5′SS selection towards *HEH1S*. Overexpression of none of these proteins increased the Heh1S isoform or suppressed the Heh1L (Supplementary Fig. 1m, n). Even Hub1's constitutive presence in the spliceosome through its chromosomal fusions to two *HEH1S* splicing-promoting factors, Snu66 and Prp38, could not alter the Heh1S/Heh1L ratio (Supplementary Fig. 1o). Since excess trans-acting proteins could not modulate the spliceosome towards *HEH1S* site, we next asked how were the competing 5′SS decoded?

U5 and U6 snRNAs decode pre-mRNA cis elements for alternative 5′SS selection

From the splicing reporters discussed above, and known binding sites of U1, U5, and U6 snRNAs at exon-intron boundaries, we narrowed a 16-nucleotide pre-mRNA segment (1913–1928 of the *HEH1* gene) and studied its importance for alternative 5′SS selection by mutagenesis (Fig. 2a). Proteins originating from the variants were detected by western blots, and mRNAs by RT-PCR followed by cDNA sequencing (Fig. 2b, c). Almost any change in this segment lost alternative splicing (barring the G(−1)A variant of *HEH1S*) and produced either one of the Heh1 isoforms. Changes leading to stop codons were studied by cDNA sequencing. GCAA to GUAA change of the upstream 5′SS gains an in-frame stop codon of *HEH1L* mRNA, abolishing the Heh1L protein (this

https://doi.org/10.1038/s41467-025-67659-8

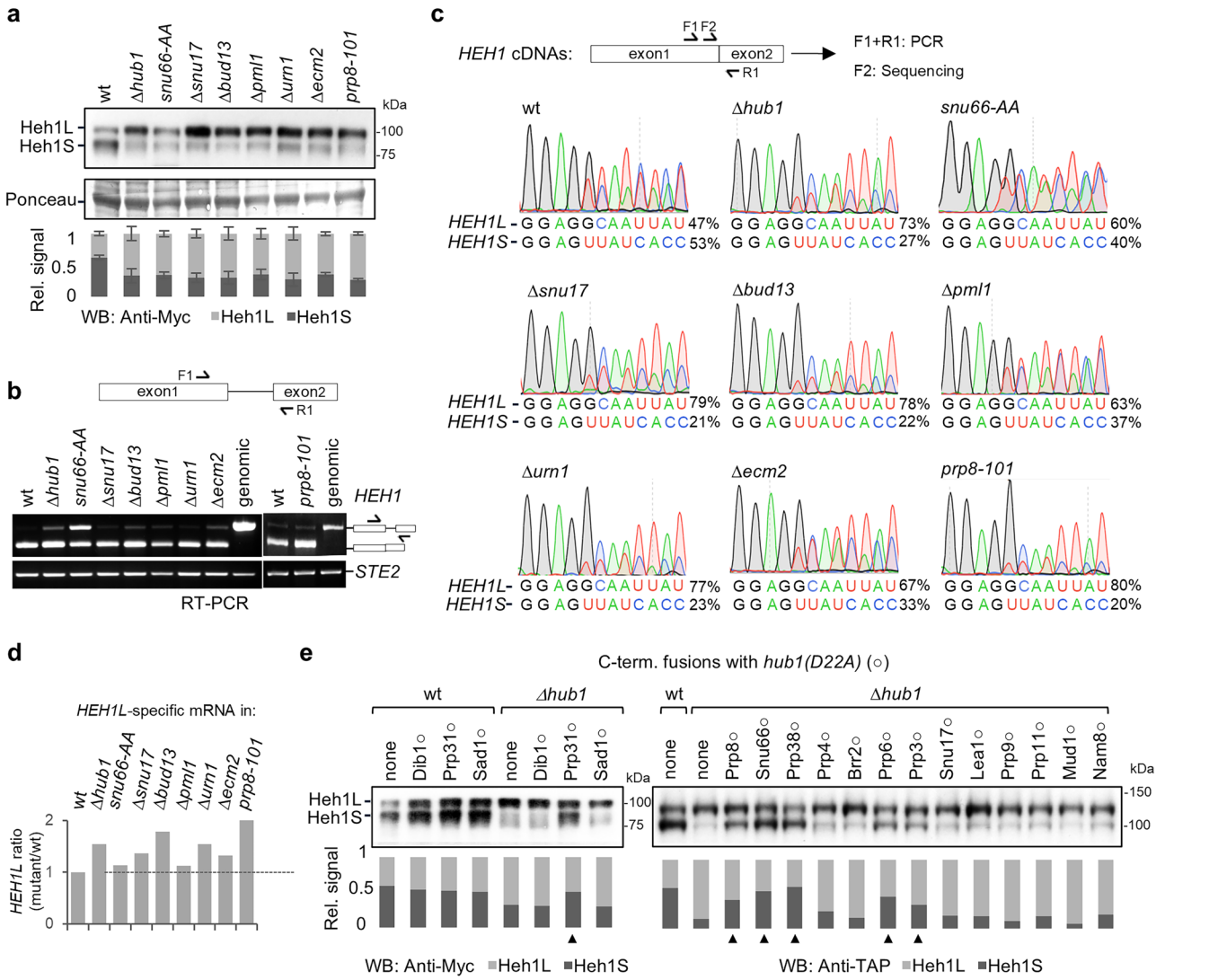

Fig. 1 | *HEH1* alternative splicing needs B and Bact proteins. a The abundance of Heh1L and Heh1S protein isoforms in the mutants of the indicated spliceosomal proteins was monitored by western blots. *hub1*, *snu17*, *ecm2*, and *urn1* mutant strains are respective gene knockouts. *snu66-AA* mutant refers to R16A and R47A variant of Snu66, its Hub1-binding-deficient HIND mutant. *prp8-101* is the E1960K allele of Prp8. The mutants were identified in targeted screens shown in Supplementary Fig. 1b-l. Data shown as mean ± s.d. ($n = 3$ independent replicates). **b** RT-PCR assays using primers F1 and R1 to monitor *HEH1* pre-mRNA splicing in the mutant strains. **c** Spliced cDNA bands were purified from mutants in (b) and sequenced with a nested F2 primer to estimate the extent of *HEH1* alternative splicing from the area under the peaks of isoform-specific nucleotides. The values for UUAUCACC indicate the relative abundance of *HEH1S*, and for GCAAUUAU show the relative abundance of *HEH1L*. The peak for the underlined 'A', being common to both isoforms, was omitted from the quantitation. The values on the right of the peaks indicate the relative abundance of respective mRNA isoforms. **d** The relative abundance of *HEH1L* mRNA in different strains was estimated from the cDNA electropherogram in (**c**). **e** Splicing factors from distinct spliceosomal complexes were probed by linear chromosomal fusions of a Snu66-binding-deficient *hub1(D22A)* mutant (indicated with empty circles) at the C-termini of respective splicing factors. Rescue of alternative splicing defects (gain of Heh1S protein) following *hub1(D22A)* fusion in the *Δhub1* background was monitored in Western blots. Note that the otherwise free *hub1(D22A)* is deficient in *HEH1* alternative splicing[13] (also see Supplementary Fig. 1g, h). Upward triangle marks *Δhub1* strain harbouring splicing factor–*hub1(D22A)* fusions, where Heh1S protein was restored.

data explains the choice of the 'GC' donor for *HEH1S* splicing; a 'GU' would have abolished Heh1L). These results highlighted the invariability of nucleotides around the competing 5′SS.

The alternative splicing defects in the pre-mRNA variants, however, did not correlate with predicted U1 snRNA–5′SS interactions. Although U1 snRNA-*HEH1S* 5′SS pairing was weaker in *HEH1* pre-mRNA variants #4, #7, #11, and #13, Heh1S protein remained unaffected. Similarly, Heh1L expression did not diminish with weakened U1 pairing of #9, #12, and #14. Strikingly, we noticed a perfect correlation in the 5′SS choice and their expected base-pairing strengths with U5 and U6 snRNAs. 5′SS that paired stronger to U5 or U6 snRNAs was the preferred donor, and the use of the second site was minimal (Fig. 2 and Supplementary Fig. 2).

U5 and U6 snRNAs can promote alternative 5′SS selection without the protein factors

From Fig. 2, U5 and U6 (but not U1) snRNA variants with modified base pairing to the competing sites were expected to bias the selection. Indeed, the respective 5′SS was used more efficiently upon overexpression of U5 and U6 snRNA variants with strengthened base pairing (Fig. 3b). Similar overexpression of the U1 snRNA variant did not alter 5′SS choice. U5 snRNA U(98)G and U6 snRNA A(45)G variants with stronger binding to *HEH1L* 5′SS increased Heh1L protein (Supplementary Fig. 3). Conversely, U5 snRNA U(98)C and U6 snRNA U(46) C A(45)U variants with stronger binding to *HEH1S* 5′SS increased Heh1S mRNA and protein (Fig. 3b, c and Supplementary Fig. 3a, b, e, f). Thus, the 46th and 45th nucleotides of U6 snRNA, beyond the ACAGA box,

https://doi.org/10.1038/s41467-025-67659-8

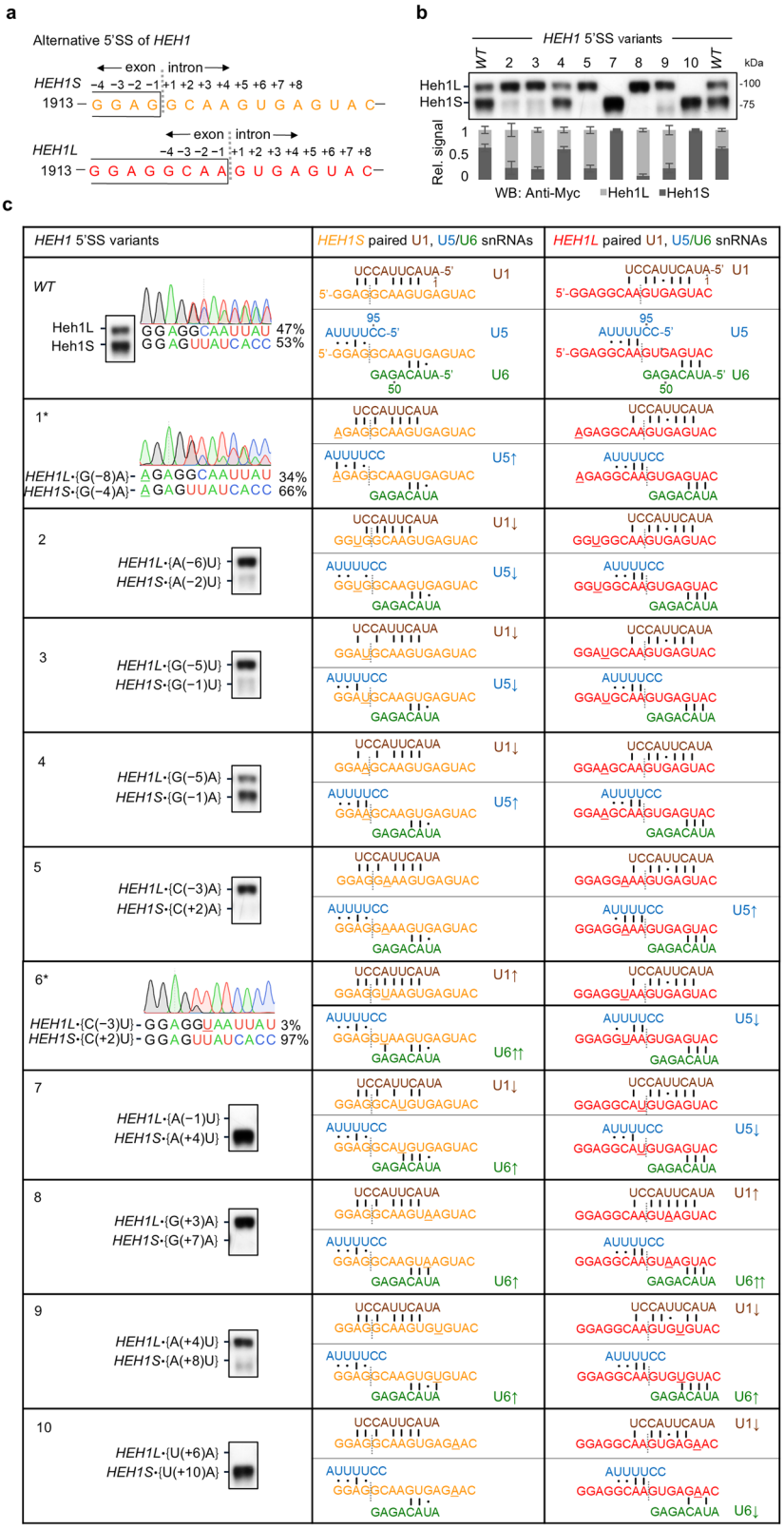

were also crucial for selecting the alternative 5'SS by base pairing at +7 and +8 nucleotides in the intron.

If the proteins discussed above act by stabilising U5 and U6 snRNAs on the pre-mRNA substrate, the snRNA variants pairing strongly to *HEH1S* 5'SS should bypass the need for the proteins. Indeed, overexpression of U(98)C variant of U5 snRNA and U(46)C, A(45)U variants of U6 snRNA restored alternative splicing defects in Δ*hub1*, Δ*snu17*, Δ*ecm2*, and Δ*urn1* mutants (Fig. 3 and Supplementary Fig. 3). Notably, the defect in *prp8-101* strain was partially restored by overexpression of the U5 and U6 snRNA variants, suggesting an additional role of the core spliceosome protein Prp8 in 5'SS selection.

Fig. 2 | Sequence at the exon-intron boundary of *HEH1* determines alternative 5′SS selection. a The 16-nucleotide segment at the exon/intron (1913–1928) boundary of *HEH1* was investigated for alternative splicing by mutagenesis. The sequence was selected based on the pairing of U1 snRNA, U5 snRNA loop 1, and U6 snRNA ACAGA box. *HEH1S* (orange) and *HEH1L* (red) sequences represent *HEH1* pre-mRNA isoforms. **b** The *HEH1* gene was mutated by site-directed mutagenesis, sequentially from left to right (except for the essential 'G' of the splicing donors), and alternative selection was monitored by western blot. Heh1 isoforms in wt yeast are used as the reference for alternative splicing. Data shown as mean ± s.d. ($n = 3$ independent repeats). **c** Analysis of pre-mRNA variants pairing with U1 snRNA (brown), U5 snRNA (blue) and U6 snRNA (green) for both *HEH1S* and *HEH1L* is tabulated. The mutants were analyzed for presumed pairings with U1, U5, and U6 snRNAs, adapted from[73–75]. Nucleotide changes are underlined. Western blot lanes are taken from (**b**). The number in the left column shows the ID of the *HEH1* variant. The changes for *HEH1S* and *HEH1L* are shown in curly brackets. Filled dots show non-Watson-Crick pairing, standing lines represent Watson-Crick pairing, upward arrows indicate the increase in U5 and U6 pairing compared to WT *HEH1S* or *HEH1L*, downward arrows show the decrease in U5 and U6 pairing compared to WT, and double upward arrows represent changes resulting in canonical 5′SS for yeast (GUAUGU or GUAAGU). The underlined nucleotides show mutation sites. The variants leading to premature stop codons, indicated by an asterisk, could be analysed only by cDNA sequencing. The values on the right of the peaks indicate the relative abundance of respective mRNA isoforms.

The Prp8-101 surface is critical for processing the 'GC' donor

Prp8 is reported to exist in two distinct conformations to maintain equilibrium between the two catalytic steps of splicing; consequently, two opposing alleles of Prp8 rescue splicing defects in one another[45]. Among the three first-step alleles of Prp8 (101, syf77, and R1753K; Supplementary Fig. 4c), only *prp8-101* showed defective *HEH1* alternative splicing. Combining the second step Prp8 alleles, *prp8-161* and *prp8-162*, with *prp8-101* did not restore the defects (Supplementary Fig. 4d, e). Thus, the alternative splicing defects in the first-step Prp8 allele, *prp8-101*, could not be explained by the above mechanism.

In a pre-mRNA variant (#7), the upstream 5′SS/GCAUGU with 'GC' donor was preferred over the downstream /GUGAGU in wt, Δ*hub1*, Δ*snu17*, Δ*ecm2*, and Δ*urn1* strains (Fig. 4b and Supplementary Fig. 4b), likely due to the stronger pairing of +4U with the ACAGA box of U6 snRNA. However, the *prp8-101* allele could not use this site. The defect in *prp8-101* was explored using the *ACT1–CUP1* splicing reporter with a single 5′SS[46]. The 5′SS/GCAUGU was used efficiently in all mutants, except for Δ*hub1* and *prp8-101*. C(+2)U-exchanged /GUAUGU was efficiently used in all strains, including Δ*hub1* and *prp8-101* (Fig. 4c). Thus, the donor with +2C was poorly used in *prp8-101* and Δ*hub1*, leading to the loss of alternative splicing. Similarly, splicing from a + 3 C 5′SS variant /GUCUGU was defective in Δ*hub1*, Δ*snu66*, and *prp8-101* strains (Supplementary Fig. 4f). Thus, the Prp8-101 surface promotes selection (and catalysis?) from non-canonical 5′SS containing +2C and +3C.

Specific competing 5′SS allow alternative splicing without the regulatory proteins

Optimal decoding of competing 5′SS by U5 and U6 snRNAs, together with the use of 'GC' donor by Prp8, is the primary determinant of alternative splicing. The process is facilitated by specific proteins of the spliceosome. Thus, competing 5′SS with modified binding to the snRNAs should allow alternative selection in the absence of the regulatory proteins. More pre-mRNA variants were assayed to identify such 5′SS.

Two 5′SS variants allowed alternative splicing not only in wt yeast (Supplementary Fig. 2) but also in strains mutated for the regulatory proteins (Fig. 4b and Supplementary Fig. 4b). U5 and U6 snRNAs' base pairing was recalibrated in #15 with two non-canonical 5′SS/GCAA/GUAUAU. In contrast, 5′SS pairing with U6 snRNAs was strongest in #18, containing two canonical 5′SS/GUAU/GUAUGU. The sites being canonical were readily used without the need for the protein factors, including the Prp8-101 surface. The efficient use of canonical 5′SS in the absence of the protein factors was further supported by *HEH1–CUP1* reporters (Supplementary Fig. 4g–i).

Ecm2, Urn1, and the RES proteins bring the weaker 5′SS into competition

HEH1S expression from /GCAA/GUAUAU 5′SS (#15) in cells lacking the protein factors was intriguing, since the changes in this variant were beyond the hexanucleotide /GCAAGU. The outcomes could be explained by two possibilities: (i) weakening of the *HEH1L* 5′SS /GUGAGU to /GUAUAU rebalanced the competition in favour of the *HEH1S* site, or (ii) improved binding of +7A and +8U in /GCAAGUAU to U6 snRNA nucleotides U46 and A45 favoured the *HEH1S* 5′SS. To study these possibilities, alternative splicing reporters, *HEH1S–CUP1* and *HEH1L–CUP1*, were made (Fig. 5b).

HEH1L 5′SS was weakened into /GUGAGA (#10; it also lacks potential *HEH1S*-U6 pairing at +7 and +8 positions) or /GUAUAA (#20; with enhanced U6 pairing at +7 and +8 positions of *HEH1S*) (Fig. 5a, c). *HEH1S* 5′SS selection in Δ*hub1* improved for reporters with enhanced U6 pairing at +7 and +8 positions of the 5′SS, and the defect was partially restored in the *prp8-101* allele. The data confirmed the importance of U6 snRNA's U46 and A45 nucleotides for alternative splicing discussed earlier in Fig. 3. The 5′SS selection in Δ*snu17*, Δ*urn1*, and Δ*ecm2*, on the other hand, was improved by both enhanced U6 snRNA pairing to *HEH1S* and weakening the competition from *HEH1L* (Fig. 5d). Thus, Hub1 and Prp8 promote selection of 5′SS with +2C by stabilising U5 and U6 snRNA on the target pre-mRNA. On the contrary, Snu17, Urn1, and Ecm2 promote competition for the weaker 5′SS by stabilising snRNA–pre-mRNA interactions.

The data presented support dominant roles of U5 and U6 snRNAs and regulatory roles of B and Bact proteins for the selection of competing 5′SS in *HEH1* pre-mRNA (Fig. 6).

Discussion

The competing 5′SS of yeast *HEH1* are decoded for alternative splicing by U5 and U6 snRNAs during the B to Bact transition of the spliceosome. The mechanism is likely to be conserved for closely-placed 5′SS in other eukaryotes. The 'GC' dinucleotide donor is found in nearly 1% introns in human[11], and the trans-acting proteins supporting its selection in yeast are conserved across eukaryotes. At the B stage of the spliceosome, U1 snRNA hands over the 5′SS to U6 snRNA via Prp28. The ACAGA box of U6 base pairs with +3 to +6 nucleotides of the 5′SS, and U5 snRNA's loop 1 base pairs with the upstream four nucleotides of the exon[33,47]. Besides its ACAGA box, the 45th and 46th nucleotides of U6 snRNA played critical roles in alternative splicing through base pairing with +7 and +8 positions of *HEH1* 5′SS. This observation underlined the importance of +7 and +8 intronic nucleotides for the first catalytic step reported earlier[48].

Strikingly, early splicing factors of U1 and U2 snRNPs were not critical for *HEH1* alternative splicing, suggesting a normal recognition of the intron. Instead, the two 5′SS were possibly handed over to U5 and U6 snRNAs differently, and their pairing strengths determined the 5′SS choice. Indeed, optimal pairing strengths of U5 and U6 snRNAs, but not of U1 snRNA, to the competing sites decided the choice of 5′SS. Any deviations led to the loss of alternative splicing and resulted in the production of the *HEH1* isoform, which exhibited improved snRNAs–pre-mRNA interaction. U5 and U6 snRNA variants with reinforced pairing to the *HEH1S* site not only favoured its selection in wt but also rescued the defects in yeast lacking the trans-acting proteins. Furthermore, pre-mRNA variants with recalibrated U5 and U6 snRNA pairing to the competing 5′SS were alternatively spliced in the absence of the trans-acting proteins.

https://doi.org/10.1038/s41467-025-67659-8

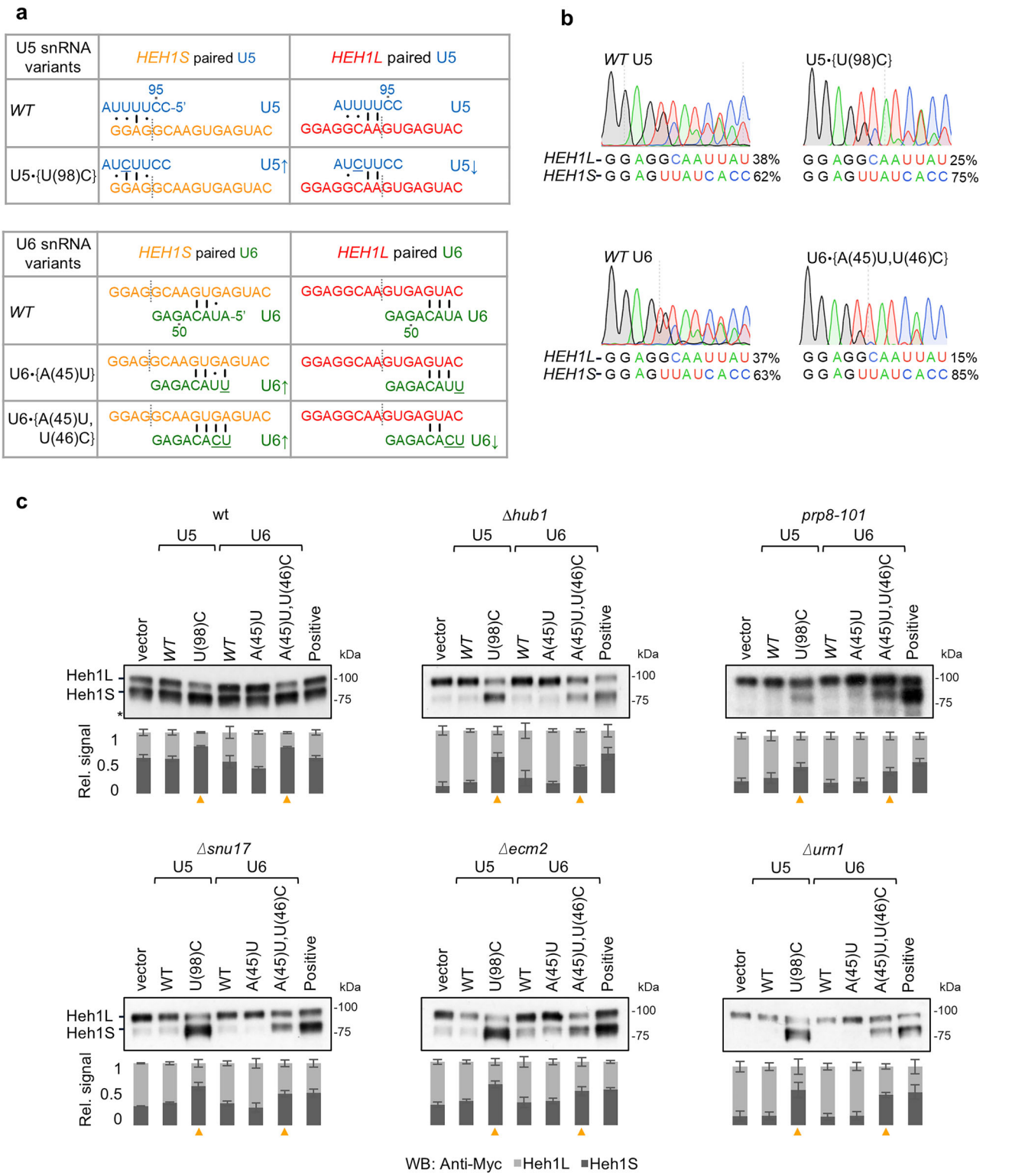

Fig. 3 | Role of U5/U6 pairing to competing 5′SS. a The pairing of U5 snRNA and its variant U5•{U(98)C} and U6 snRNA and its variant U6•{A(45)U,U(46)C} to *HEH1* pre-mRNA. The snRNA variants were identified (Supplementary Fig 3a, b, e, f) by mutagenesis of U5 Loop 1 and U6 ACAGA box. Nucleotide changes are underlined. Upward/downward arrows refer to an increase/decrease in U5/U6 pairing strength to *HEH1* isoforms. *HEH1* mRNA and proteins were assayed after overexpressing U5 and U6 snRNA variants under respective promoters and terminators from multi-copy plasmids. **b** *HEH1* cDNAs from yeast strains overexpressing U5 and U6 snRNAs and their variants were sequenced to monitor alternative 5′SS selection. Area under the peak was integrated (similar to Fig. 1) to estimate the relative abundance of the two mRNA isoforms. The values on the right of the peaks indicate the relative abundance of respective mRNA isoforms. **c** The expression of Heh1 protein isoforms upon overexpression of U5 and U6 snRNA variants, monitored in different mutants by western blots. Heh1 isoforms in wt yeast (labelled as 'Positive') are used as the reference for alternative splicing. Data shown as mean ± s.d. ($n = 3$ independent replicates). Orange upward triangles indicate snRNA overexpression, resulting in relatively higher amounts of Heh1S protein in wt, and its rescue in the mutant strains.

https://doi.org/10.1038/s41467-025-67659-8

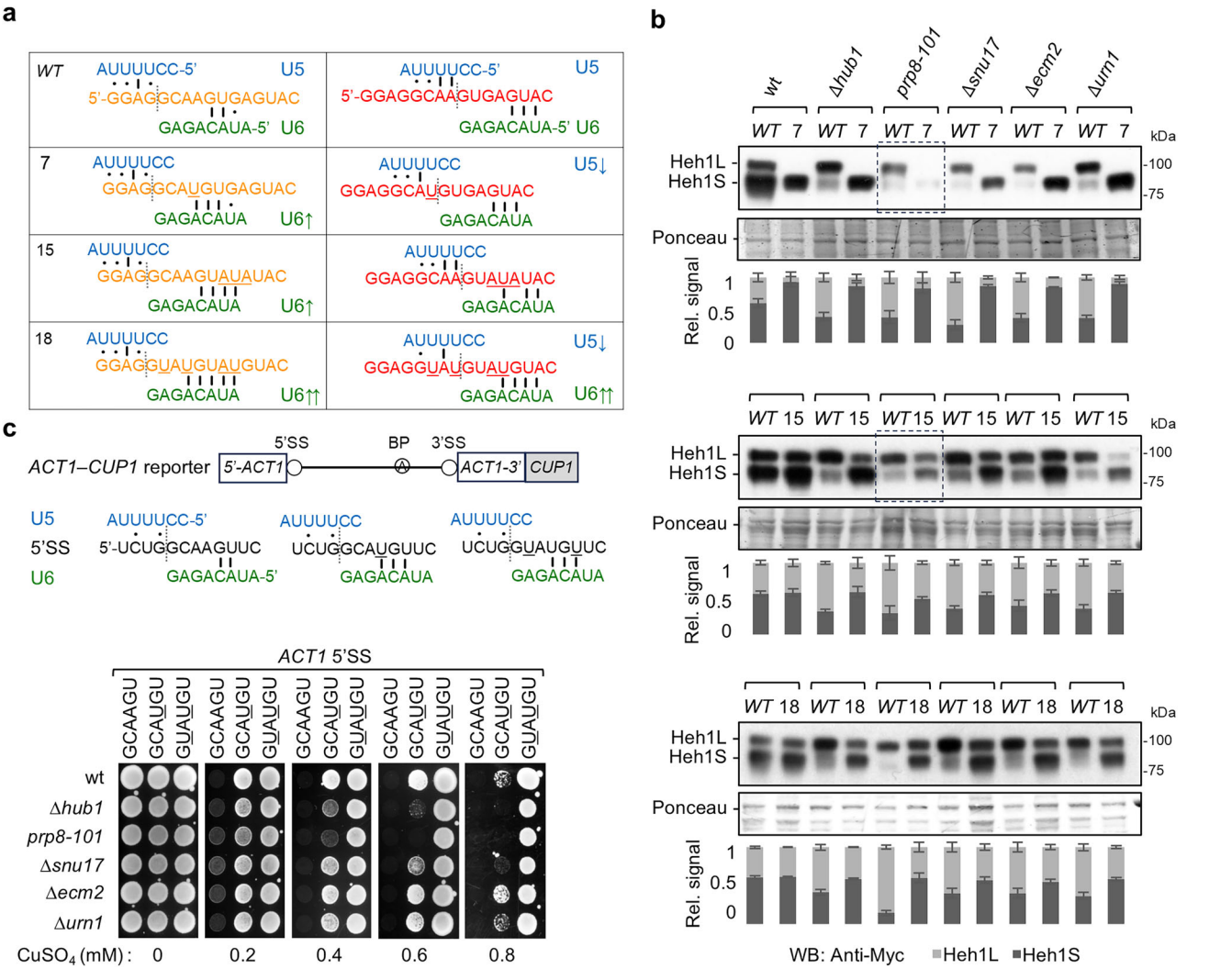

Fig. 4 | The protein factors are dispensable for alternative splicing from specific 5′SS variants. a Pairing of U5 and U6 snRNAs to *HEH1 WT* pre-mRNA and its variants #7 *HEH1S*•{A(+4)U} or *HEH1L*•{A(−1)U}; #15 {*HEH1S*•{G(+7)A,A(+8)U,G(+9)A} or *HEH1L*•{G(+3)A,A(+4)U,G(+5)A}; and #18 *HEH1S*•{C(+2)U,A(+4)U,G(+7)A,A(+8)U} or *HEH1L*•{C(−3)U,A(−1)U,G(+3)A,A(+4)U}. Nucleotide changes are underlined. Upward/downward arrows refer to an increase/decrease in U5/U6 pairing strengths to *HEH1* isoforms, and double upward arrows represent the yeast canonical 5′SS (GUAUGU or GUAAGU). **b** Alternative splicing of *HEH1* variants #7, 15, and 18 was analyzed in the mutant strains by western blot. Partial rescue of Heh1S in the *prp8-101* strain is shown in the dotted box. Data shown as mean ± s.d. ($n = 3$ independent repeats). **c** *ACT1–CUP1* reporter with a single 5′SS was used to understand the exclusive production of Heh1S from #7 {A(+4)U}. U5 and U6 snRNAs pairing to *HEH1S* 5′SS GCAAGU, GCAUGU, and GUAUGU were compared by growth at indicated $CuSO_4$ concentrations (in mM), which correlates with their splicing efficiency. The underlined nucleotides show changes compared to the *HEH1S* 5′SS GCAAGU.

The proteins critical for the alternative selection of *HEH1* 5′SS reported earlier[13] and identified in this study are components of the spliceosome B and Bact complexes. Importantly, alternative 5′SS of *HEH1* is the first in vivo target of these proteins, including the *prp8-101* allele, in *S. cerevisiae*. The proteins appear to facilitate alternative 5′SS selection by stabilising the spliceosome in a low-fidelity, high-efficiency conformation on the weaker site. Supporting this proposition, the Hub1-Snu66 complex enhances the selection of non-canonical 5′SS and promotes error-prone splicing[13,40]. the RES complex proteins Snu17, Bud13, and Urn1 promote non-canonical splicing[49–51], and the NTC subunit Ecm2 facilitates the selection of non-canonical and competing 5′SS[52]. The proteins seem to promote competition for the alternative 5′SS in *HEH1* at the expense of the dominant site. The selection *HEH1S* site needed these proteins, but in their absence, the *HEH1L* site was chosen better, possibly due to the loss of competition.

Hub1 joins the spliceosome through non-covalent associations with Prp5 and Snu66. The D22A surface of Hub1 binds Snu66 in multiple eukaryotes[13,53–55]. Interestingly. the same Hub1 surface binds MFAP1 (Spp381 in yeast) in the human B spliceosome[43,44]. The D21 residue of Hub1 also interacts with the same surface of MFAP1[43]. An additional RNA-binding surface of Hub1, comprising N7 and K13 residues, is reported to bind the 5′ exon at −3 and −4 positions in human spliceosomes[44], was also critical for *HEH1* alternative 5′SS selection. Thus, Hub1 may be recruited to the early B complex through Snu66-HIND[13] and promotes alternative 5′SS selection, possibly after switching to the pre-mRNA and MFAP1 in the late B complex[43,44].

The role of U4/U6 proteins, Prp3, Prp6 and Prp31, in alternative 5′SS selection was revealed through proximity probing with Hub1. These proteins surround the core Prp8 and undergo a major switch during the conversion of pre-B to B. The 180° shift in Prp8's RNaseH/RH domain with the associated factors[43,56] appears to be important for the recognition of *HEH1* alternative 5′SS. Snu66 along with Prp3, Prp6 and Prp31 stabilise U4/U6 binding and prevent premature Brr2 helicase activity[57,58]. Prp38, Snu23, and Spp381 (also called B complex proteins or BCP) form a module that interacts with Prp8 and positions Brr2

https://doi.org/10.1038/s41467-025-67659-8

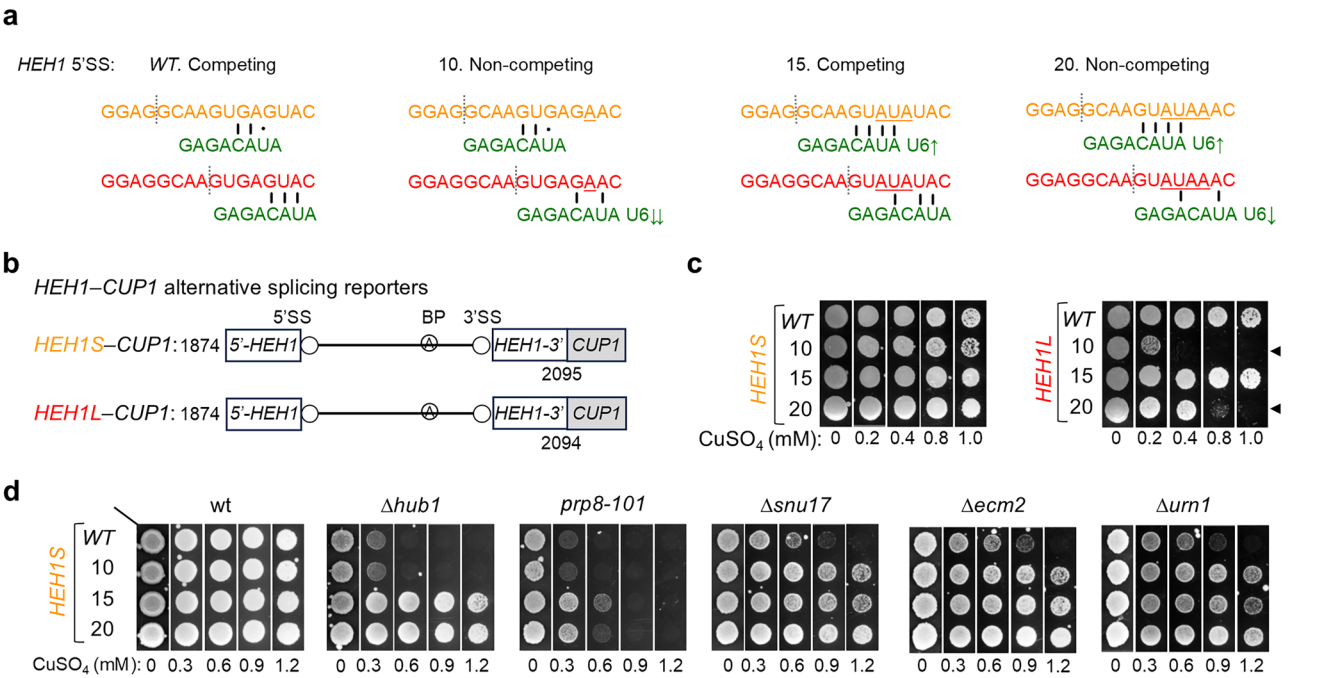

Fig. 5 | 5′SS competition versus U6 snRNA pairing. a Pairing of U6 snRNA with *HEH1 WT* pre-mRNA, variant #10 *HEH1S*•{U(+10)A} or *HEH1L*•{U(+6)A}; #15 {*HEH1S*•{G(+7)A,A(+8)U,G(+9)A} or *HEH1L*•{G(+3)A,A(+4)U,G(+5)A}; and #20 {*HEH1S*•{G(+7)A,A(+8)U,G(+9)A,U(+10)A} or *HEH1L*•{G(+3)A,A(+4)U,G(+5)A,U(+6)A}. Upward/downward arrows indicate an increase/decrease in U6 pairings and competition between the two 5′SS. Nucleotide changes are underlined. **b** *HEH1–CUP1* alternative splicing reporters made by replacing the *ACT1* part with the *HEH1* segment in the *ACT1–CUP1* reporter. The *HEH1* segment used for *HEH1S–CUP1* was 1874-2095 and for *HEH1L–CUP1* 1874-2094. In *HEH1S–CUP1, HEH1S* mRNA is in frame with *CUP1*, and in *HEH1L–CUP1, HEH1L* mRNA is in frame with *CUP1*. **c** Reporter activities were tested at different $CuSO_4$ concentrations. The left-pointed triangle denotes the *HEH1L*-abolished 5′SS in #10 and the *HEH1L*-weakened site in #20. Mutated *HEH1L* 5′SS do not compete with the *HEH1S* site. **d** The *HEH1S–CUP1* reporter variants were tested for their splicing efficiency by yeast growth at different $CuSO_4$ concentrations. Loss of competition restored splicing from *HEH1S* 5′SS in *snu17, ecm2* and *urn1* mutants, but not in *hub1* and *prp8-101* mutants. Gain of U6 snRNA pairing at +7 and +8 positions of *HEH1S* 5′SS restored splicing defects, fully in most mutant strains and partially in *prp8-101*.

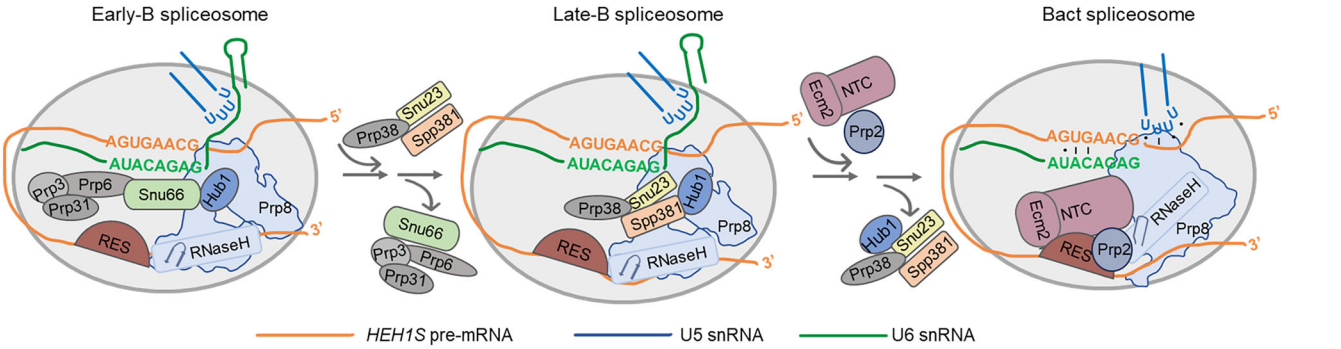

Fig. 6 | Plausible mechanism of *HEH1* alternative 5′SS selection. The schematics show changes from B to Bact complex during selection of the alternative *HEH1* 5′SS. Snu66 escorts Hub1 to the 5′ exon in the early B complex, and hands over to the Spp381/MFAP1 (a subunit of the Prp38 complex)[43,44] in the late B complex. Thus, Hub1 binding to Snu66 and Spp381/MFAP1 may be mutually exclusive. Hub1 also binds RNA at the 5′ exon near the exon-intron boundary. The tri-snRNP factors Prp6, Prp3 and Prp31 are present throughout the B complex. They likely stabilise the U4/U6 snRNA duplex and prevent its premature unwinding[76]. Prp8 is converted from a partially open conformation to a closed state during the transition from B to Bact states[66,73]. The changes in the Prp8 RH domain, during β-hairpin to loop conformation, orchestrate the release of tri-snRNP factors and incorporation of NTC into the spliceosome[64,73].

helicase for the unwinding of U4/U6 RNA duplexes, resulting in the release of Snu66, Prp3, Prp6, Prp31 and U4 snRNP. Moreover, the NTC protein gets incorporated into the B complex, which triggers the release of BCP[59], U6 snRNA forms new interactions with U2 snRNA, assembling the catalytic core. The NTC protein Ecm2 and the RES complex proteins are associated with the Bact complex, highlighting the role of the RES in the remodelling of Bact via Prp2. The RES complex leaves the spliceosome during Bact to B* conversion[60,61].

Among the fourteen Prp8 alleles[62] tested here, the *prp8-101* (E1960K) mutant[63], which lies in the RH domain, was defective in selecting the alternative 5′SS. The RH domain toggles between transitional and catalytic conformations[64]. It remains in a partially closed conformation until the B complex and promotes splicing fidelity over efficiency. Prp8's first-step alleles[65] and Prp38[66] have been shown to stabilise the high-fidelity conformation. The marking of the pre-mRNA target by the snRNAs in the B complex induces U4/U6 snRNA unwinding and concomitant U2/U6 snRNA pairing in the Bact

complex[67]. The RH domain switches to a completely closed conformation in the Bact complex[60,64] and positions the target pre-mRNA for first-step catalysis. The switch may define the branching site for the first catalytic step for the +2C-containing *HEH1* 5′SS in the B* complex, likely with the help of the Prp8-101 surface. The defective splicing in *prp8-101* from +2C and +3C containing 5′SS suggests a high-fidelity, low-efficiency nature of this mutant, and the role of Prp8 in selection (or catalysis) of +2C and +3C containing 5′SS. In contrast to the full rescue of *HEH1* alternative splicing observed upon overexpression of U5 and U6 snRNA variants in the deletion of other splicing proteins, the partial rescue of *prp8-101* defects points to a potential role of this Prp8 surface in catalysis from the 'GC' donor.

In conclusion, yeast *HEH1/SRC1* pre-mRNA is an important substrate for studying alternative splicing through competing 5′SS. RNA-RNA interactions are central to alternative splicing through competing 5′SS, but early recognition factors are dispensable for the selection of the closely-spaced 5′SS. Evidences presented here, along with the literature, support a plausible mechanism of alternative 5′SS selection in the B and Bact spliceosomes orchestrated by U5 and U6 snRNAs as the primary determinants and not the U1snRNPs. Splicing factors promoting selection of weak 5′SS, reported previously (Hub1, Snu66, Prp38, Prp8), and identified in this study (the B complex proteins Prp3, Prp6, Prp31, and Snu66; the RES complex subunits Bud13, Snu17, Pml1 and Urn1, and the NTC complex Ecm2) function through the B or Bact spliceosomes. U5 and U6 snRNAs are essential components of both these assemblies. With the help of the trans-acting proteins, U5 and U6 snRNAs pair with the target pre-mRNA for alternative 5′SS selection and catalysis.

Methods

Reagents

All the reagents and software used in the study are listed in Supplementary Table 1.

Plasmids, *S. cerevisiae* strains, yeast transformation and growth assays

Plasmids and strains used in this study are listed in Supplementary Tables 2, 3, respectively. The yJU75 yeast strain, plasmids *PRP8* and *prp8-101*, and *ACT1–CUP1* reporter were kind gifts from C. Guthrie and M. Konarska's lab. Prp8 mutant strains were made by shuffling out the Ura+ *PRP8* wild-type plasmid with the Trp+ *prp8* mutants on 5-fluoroorotic acid (FOA) plates. *The S. cerevisiae* deletion strains of splicing factors were obtained from the Euroscarf haploid deletion library. Competent cell preparation and transformation were performed following previously published protocols.[68,69]. Chromosomal tagging for western blot, double knockout strains for genetic interactions, and splicing factors deletion in the yJU75 background were made by using the reported protocol.[68,69]. Protein overexpression was achieved by expressing clones under a strong *gal promoter*. For growth/spot assays, fivefold serial dilutions of cells were spotted on the indicated agar plates, and plates were incubated at the temperatures indicated in the figure.

Chromosomal fusion of *hub1–D22A* to the C-termini of splicing factors

Splicing by overlap extension (SOE) PCR was done to make *hub1(D22A)* C-terminal fusion to essential splicing factors. This fusion was done based on the published protocol[68]. Three sets of primers were used to amplify three fragments. First set of primers amplified a 200–300 bp fragment of the C termini of the desired gene, excluding the stop codon. The reverse primer of this had an overhang of 20–25 bps that was complementary to the 20–25 bps of *hub1(D22A)* N-terminus. The second set of primers amplified the full-length *hub1(D22A)* with the Nat antibiotic selection marker cassette from the plasmid clones of pFA6a-*hub1(D22A)-natNT2*. The third set of primers amplified a fragment of 200–300 bp from the stop codon of the gene that was going to be tagged. The forward primer for this had an overhang of 20–25 bp with the end of the antibiotic-resistance marker. All three fragments were amplified using Vent DNA polymerase. These fragments were confirmed based on their size on the agarose gel, and the correct fragments were gel-purified. All three fragments were mixed and joined by SOE PCR using Vent DNA polymerase using the forward primer of the first fragment and the reverse primer of the third fragment. The joined fragment was confirmed by agarose gel electrophoresis and transformed into the *S. cerevisiae* strain. The transformants were selected on agar plates with an antibiotic. The chromosomal fusion was confirmed by colony PCR using a forward primer specific to the gene and a reverse primer specific to the antibiotic cassette.

Splicing reporters

The splicing reporters used in this study are listed in Supplementary Table 4. Splicing reporters are modified forms of the conventional *ACT1–CUP1*[46] and *RP51–LACZ*[42]. The *HEH1S–CUP1* reporters have a 121 bp segment of the S. cerevisiae *HEH1* gene (1874-2095 nucleotides), including the intron, using BamHI and KpnI restriction sites. The *HEH1S* mRNA is spliced using GCAAGU 5′SS, generating in-frame *CUP1* mRNA for translation. The methionine initiation codon was introduced by inserting a point mutation at C1881G. Initiation codon and variants of the 5′SS were made by site-directed mutagenesis (SDM) using specific primers, and the change was confirmed using Sanger sequencing. For *HEH1L–CUP1* reporter, a 120 bp segment of the *HEH1* gene (1874-2094 nucleotides) was used to bring the *HEH1L* mRNA spliced using GUGAGU 5′SS in-frame with the *CUP1* gene. For reporter assays, competent cells from the *S. cerevisiae* strain yJU75 were transformed with the reporters, and transformants were selected in media lacking leucine. 1 OD_{600} cells were spotted on solid media with different concentrations of $CuSO_4$. The plates were incubated for 2–3 days at 30 °C. Similarly, for *HEH1–LACZ* reporters, the *RP51* part of the *RP51–LACZ* reporter (gift from M. Rosbash) was replaced with a *HEH1* fragment of 399 bp (1792-2191 nucleotides) and 398 bp (1792-2190 nucleotides) to obtain *HEH1S–LACZ* and *HEH1L–LACZ* reporters, respectively.

β-galactosidase assay

β-galactosidase activity was observed on both solid and liquid media. The X-gal overlay and the ONPG assay were performed by following published protocols[70].

RNA isolation and cDNA synthesis

RNA isolation and cDNA synthesis were done as described previously[71]. Briefly, five OD_{600} cells in the log phase were harvested. Total RNA was isolated by the hot acid phenol method using 15 mL phase lock tubes for phase separation. Residual DNA was removed by treating RNA with DNase I for 15 min at room temperature, followed by RNA clean-up using a Zymo-Spin™ II column. cDNA synthesis from 2 µg total RNA was done using reverse transcriptase (RT) and random-hexamer primers at 37 °C for 2 h. Splicing defects were monitored by detecting intron-containing transcripts or post-splicing mature transcripts using exonic primers across the intron and analysed by agarose gel electrophoresis. For cDNA sequencing, five identical PCR reactions were performed. The PCR products were pooled and kept overnight for precipitation after adding 2.5 times the volume of isopropanol and 1/10th the volume of 3 M sodium acetate at −20 °C. DNA was pelleted by centrifugation for 15 min at 4 °C at maximum speed. The pellet was washed twice with 70% ethanol. Dried pellets were dissolved in 30 µl of nuclease-free water, and 10 µl of the DNA was sequenced by Sanger sequencing using a primer nested inside the forward primer used in amplification.

Quantification of *HEH1* mRNA isoforms

HEH1 alternative splicing was analysed using RT-PCR followed by cDNA sequencing. We have two sets of primers. To check the splicing defect,

we have used the F1 and R1 primers. We have cut the mRNA band (the lower one) and gel-purified it. We have used F2, which is nested in the F1 primer and R1, for reamplifying the mRNA band. We did ethanol precipitation of the PCR product and sent it for Sanger sequencing using the F2 primer. The primer sequences are listed in Supplementary Table 5.

HEH1S and *HEH1L* mRNAs differ in GCAA nucleotides at their exon junctions (*HEHL* gains them due to the usage of downstream 5′SS), the electropherogram shows mixed peaks corresponding to the two isoforms after the exon-exon junction. The area under the peaks was integrated to find the relative abundance of the two mRNAs. Both common and isoform-specific peaks were analysed within the region corresponding to the 5′exon/intron boundary. To understand alternative 5′SS usage, common nucleotides after the junction in the two isoforms were excluded from further analysis. For each site, we recorded the nucleotide proportions possible for both the cDNAs and calculated the ratio between the two nucleotides, normalising their combined total to 100%. The average value of both forms is directly related to their respective 5′SS usage.

Relative expression of *HEH1L* in wild-type and yeast mutants was obtained from the cDNA electropherogram. The areas under ten common and ten mixed peaks (before and after the junction, respectively), were integrated and averaged. Similarly, an area under the peaks specific to *HEH1L* was integrated and averaged. The ratio of common and *HEHL* peaks for different strains was obtained. The fold difference in *HEH1L* expression in the mutants was calculated against the wild-type strain by dividing the average of the area under *HEH1L* peaks (after the junction) by the average of the area under common peaks (before the junction).

Western blots

For protein western blots (immunoblotting), logarithmically growing cells equivalent to 2 OD_{600} were harvested. Whole protein was extracted using the trichloroacetic acid (TCA) method[68]. Total proteins used for Western blots were denatured by heating cells in a high-urea buffer at 65 °C for 15 min and then centrifuged. The soluble protein was separated on sodium dodecyl sulphate-polyacrylamide gel electrophoresis (SDS-PAGE) 8% gels, or NuPAGE™ 4–12% Bis-Tris gels (Invitrogen), transferred to a polyvinylidene difluoride (PVDF) membrane, and probed with specific primary and secondary antibodies. Protein bands were quantified using ImageJ following the published method[72].

Further information on experimental design is available in the Nature Research Reporting Summary linked to this article.

Reporting summary

Further information on research design is available in the Nature Portfolio Reporting Summary linked to this article.

Data availability

The data supporting the findings of this study are available from the corresponding authors upon request. The raw data underlying the figures and Supplementary Figs. are provided as a source Data file. Standard deviation, bar graph, and electropherogram values are also included within the Source Data file. A.K.B. or S.K.M. may be contacted for additional details on the protocols that support the findings of this study. Source data are provided with this paper.

References

1. Will, C. L. & Lührmann, R. Spliceosome structure and function. *Cold Spring Harb. Perspect. Biol.* **3**, 1–2 (2011).
2. Wilkinson, M. E. & Charenton, C. & Nagai, K RNA splicing by the spliceosome. *Annu. Rev. Biochem.* **89**, 46 (2020).
3. WANG, Y. et al. Mechanism of alternative splicing and its regulation. *Biomed. Rep.* **3**, 152–158 (2015).
4. Zhang, Y., Qian, J., Gu, C. & Yang, Y. Alternative splicing and cancer: a systematic review. *Signal Transduct. Target. Ther.* **6**, 78 (2021).
5. Roca, X., Krainer, A. R. & Eperon, I. C. Pick one, but be quick: 5′ splice sites and the problems of too many choices. *Genes Dev.* **27**, 129 (2013). vol.
6. Ma, P. & Xia, X. Factors affecting splicing strength of yeast genes. *Comp. Funct. Genomics* **2011**, 212146 (2011).
7. Rogozin, I. B., Carmel, L., Csuros, M. & Koonin, E. V. Origin and evolution of spliceosomal introns. *Biol. Direct* **7**, 11 (2012). vol.
8. Parker, M. T., Fica, S. M. & Simpson, G. G. RNA splicing: a split consensus reveals two major 5′ splice site classes. *Open Biol.* **15**, 240293 (2025).
9. Bortfeldt, R., Schindler, S., Szafranski, K., Schuster, S. & Holste, D. Comparative analysis of sequence features involved in the recognition of tandem splice sites. *BMC Genomics* **9**, 202 (2008).
10. Dou, Y., Fox-Walsh, K. L., Baldi, P. F. & Hertel, K. J. Genomic splice-site analysis reveals frequent alternative splicing close to the dominant splice site. *RNA* **12**, 2047–2056 (2006).
11. Sibley, C. R., Blazquez, L. & Ule, J. Lessons from non-canonical splicing. *Nat. Rev. Genet.* **17**, 407–421 (2016). vol.
12. Rodríguez-Navarro, S., Carlos Igual, J. & Pérez-Ortín, J. E. SRCI: An intron-containing yeast gene involved in sister chromatid segregation. *Yeast* **19**, 43–54 (2002).
13. Mishra, S. K. et al. Role of the ubiquitin-like protein Hub1 in splice-site usage and alternative splicing. *Nature* **474**, 173–180 (2011).
14. King, M. C., Lusk, C. P. & Blobel, G. Karyopherin-mediated import of integral inner nuclear membrane proteins. *Nature* **442**, 1003–1007 (2006).
15. Grund, S. E. et al. The inner nuclear membrane protein Src1 associates with subtelomeric genes and alters their regulated gene expression. *J. Cell Biol.* **182**, 897–910 (2008).
16. Mekhail, K., Seebacher, J., Gygi, S. P. & Moazed, D. Role for perinuclear chromosome tethering in maintenance of genome stability. *Nature* **456**, 667–670 (2008).
17. Schreiner, S. M., Koo, P. K., Zhao, Y., Mochrie, S. G. J. & King, M. C. The tethering of chromatin to the nuclear envelope supports nuclear mechanics. *Nat. Commun.* **6**, 7159 (2015).
18. Capella, M., Caballero, L. M., Pfander, B., Braun, S. & Jentsch, S. ESCRT recruitment by the S. Cerevisiae inner nuclear membrane protein Heh1 is regulated by hub1-mediated alternative splicing. *J. Cell Sci.* **133**, jcs250688 (2020).
19. Puig, O., Bragado-Nilsson, E., Koski, T. & Séraphin, B. The U1 snRNP-associated factor Luc7p affects 5′ splice site selection in yeast and human. *Nucleic Acids Res.* **35**, 5874–5885 (2007).
20. Schwer, B., Chang, J. & Shuman, S. Structure-function analysis of the 5′ end of yeast U1 snRNA highlights genetic interactions with the Msl5Mud2 branchpoint-binding complex and other spliceosome assembly factors. *Nucleic Acids Res.* **41**, 7485–7500 (2013).
21. Rösel-Hillgärtner, T. D. et al. A novel intra-U1 snRNP cross-regulation mechanism: alternative splicing switch links U1C and U1-70K expression. *PLoS Genet.* **9**, e1003856 (2013).
22. Van Der Houven Van Oordt, W., Newton, K., Screaton, G. R. & Cáceres, J. F. Role of SR protein modular domains in alternative splicing specificity in vivo. *Nucleic Acids Res.* **28**, 4822–4831 (2000). vol.
23. Eperon, I. C. et al. Selection of alternative 5 splice sites: role of U1 SnRNP and models for the antagonistic effects of SF2/ASF and HnRNP A1. *Mol. Cell. Biol.* **20**, 8303–8318 (2000). vol.
24. Shaw, S. D., Chakrabarti, S., Ghosh, G. & Krainer, A. R. Deletion of the N-terminus of SF2/ASF permits RS-domain-independent pre-mRNA splicing. *PLoS ONE* **2**, e854 (2007).
25. Zhou, Z. & Fu, X. D. Regulation of splicing by SR proteins and SR protein-specific kinases. *Chromosoma* **122**, 191–207 (2013). vol.
26. Sandhu, R., Sinha, A. & Montpetit, B. The SR-protein Npl3 is an essential component of the meiotic splicing regulatory network in

Saccharomyces cerevisiae. *Nucleic Acids Res.* **49**, 2552–2568 (2021).
27. Espinosa, S. et al. Human PRPF39 is an alternative splicing factor recruiting U1 snRNP to weak 5 'splice sites. *RNA* **29**, 97–110 (2022).
28. Kawashima, T., Douglass, S., Gabunilas, J., Pellegrini, M. & Chanfreau, G. F. Widespread Use of Non-productive Alternative Splice Sites in Saccharomyces cerevisiae. *PLoS Genet.* **10**, e1004249 (2014).
29. Black, D. L. Mechanisms of alternative pre-messenger RNA splicing. *Annu. Rev. Biochem.* **72**, 291–336 (2003).
30. Rogalska, M. E. et al. Transcriptome-wide splicing network reveals specialised regulatory functions of the core spliceosome. *Science* **386**, 551–560 (2024).
31. Dvinge, H., Guenthoer, J., Porter, P. L. & Bradley, R. K. RNA components of the spliceosome regulate tissueand cancer-specific alternative splicing. *Genome Res.* **29**, 1591–1604 (2019).
32. Cortes, J. J., Sontheimer, E. J., Seiwert, S. D., Steitz, J. A. & Steitz, J. A. Mutations in the conserved loop of human U5 SnRNA generate use of novel cryptic 5′ splice sites in vivo. *EMBO J.* **12**, 5181–5189 (1993).
33. Newman, A. & Norman, C. Mutations in yeast U5 snRNA alter the specificity of 5′ splice-site cleavage. *Cell* **65**, 115–123 (1991).
34. Hwang, D.-Y. & Cohen, J. B. U1 SnRNA promotes the selection of nearby 5′ splice sites by U6 SnRNA in mammalian cells. *Genes Dev.* **10**, 338–350 (1996).
35. Shen, A. et al. U6 snRNA m6A modification is required for accurate and efficient splicing of C. elegans and human pre-mRNAs. *Nucleic Acids Res.* **52**, 9139–9160 (2024).
36. Ishigami, Y., Ohira, T., Isokawa, Y., Suzuki, Y. & Suzuki, T. A single m6A modification in U6 snRNA diversifies exon sequence at the 5′ splice site. *Nat. Commun.* **12**, 3244 (2021).
37. Rangan, R. et al. Comprehensive analysis of Saccharomyces cerevisiae intron structures in vivo. *Nat. Struct. Mol. Biol.* **32**, 1488–1502 (2025).
38. Anil, A. T. et al. Splicing of branchpoint-distant exons is promoted by Cactin, Tls1 and the ubiquitin-fold-activated Sde2. *Nucleic Acids Res.* **50**, 10000–10014 (2022).
39. Li, H. et al. Conserved intronic secondary structures with concealed branch sites regulate alternative splicing of poison exons. *Nucleic Acids Res.* **52**, 6002–6016 (2024).
40. Karaduman, R., Chanarat, S., Pfander, B. & Jentsch, S. Error-prone splicing controlled by the ubiquitin relative Hub1. *Mol. Cell* **67**, 423–432.e4 (2017).
41. Chanarat, S. & Mishra, S. K. Emerging roles of ubiquitin-like proteins in pre-mRNA splicing. *Trends Biochem. Sci.* **43**, 896–907 (2018).
42. Jacquier, A., Rodriguez, J. R. & Rosbash, M. A quantitative analysis of the effects of 5′ junction and TACTAAC box mutants and mutant combinations on yeast MRNA splicing. *Cell* **43**, 423–430 (1985).
43. Zhang, W. et al. Structural insights into human exon-defined spliceosome prior to activation. *Cell Res.* **34**, 428–439 (2024).
44. Zhang, Z. et al. Cryo-EM analyses of dimerized spliceosomes provide new insights into the functions of B complex proteins. *EMBO J.* **43**, 1065–1088 (2024).
45. Liu, L., Query, C. C. & Konarska, M. M. Opposing classes of prp8 alleles modulate the transition between the catalytic steps of pre-mRNA splicing. *Nat. Struct. Mol. Biol.* **14**, 519–526 (2007).
46. Lesser, C. F. & Guthrie, C. Mutational analysis of pre-MRNA splicing in *Saccharomyces cerevisiae* using a sensitive new reporter gene, CUP1. *Genetics* **133**, 851–863 (1993).
47. Bai, R., Wan, R., Yan, C., Lei, J. & Shi, Y. Structures of the fully assembled *Saccharomyces Cerevisiae* spliceosome before activation. *Science* **360**, 1423–1429 (2018).
48. Staley, J. P. & Guthrie, C. An RNA switch at the 5′ splice site requires ATP and the DEAD box protein Prp28p. *Mol. Cell* **3**, 55–64 (1999).
49. Brooks, M. A. et al. Structure of the yeast Pml1 splicing factor and its integration into the RES complex. *Nucleic Acids Res.* **37**, 129–143 (2009).
50. Gottschalk, A., Bartels, C., Neubauer, G., Lührmann, R. & Fabrizio, P. A novel yeast U2 snRNP protein, Snu17p, is required for the first catalytic step of splicing and for progression of spliceosome assembly. *Mol. Cell Biol.* **21**, 3037–3046 (2001).
51. Dziembowski, A. et al. Proteomic analysis identifies a new complex required for nuclear pre-mRNA retention and splicing. *EMBO J.* **23**, 4847–4856 (2004).
52. Van Der Feltz, C. et al. *Saccharomyces cerevisiae* Ecm2 modulates the catalytic steps of pre-mRNA splicing *RNA* **27**, 591–603 (2021).
53. Ammon, T. et al. The conserved ubiquitin-like protein Hub1 plays a critical role in splicing in human cells. *J. Mol. Cell Biol.* **6**, 312–323 (2014).
54. Kolathur, K. K. et al. The ubiquitin-like protein Hub1/UBL-5 functions in pre-mRNA splicing in *Caenorhabditis elegans*. *FEBS Lett.* **597**, 448–457 (2023).
55. Varikkapulakkal, A., Pillai, B. R. & Mishra, S. K. Psr1 phosphatase regulates pre-mRNA splicing through spliceosomal B complex factor Snu66. *FEBS J.* **291**, 5455–5469 (2024).
56. Zhan, X., Yan, C., Zhang, X., Lei, J. & Shi, Y. Structures of the human pre-catalytic spliceosome and its precursor spliceosome. *Cell Res.* **28**, 1129–1140 (2018).
57. Sarka, K., Katzman, S. & Zahler, A. M. A role for SNU66 in maintaining 5′ splice site identity during spliceosome assembly. *RNA* **30**, 695–709 (2024).
58. Ulrich, A. K. C., Seeger, M., Schütze, T., Bartlick, N. & Wahl, M. C. Scaffolding in the Spliceosome via Single α Helices. *Structure* **24**, 1972–1983 (2016).
59. Fu, X. & Hoskins, A. A. Dynamics and evolutionary conservation of B complex protein recruitment during spliceosome activation. *Nucleic Acids Res.* **53**, gkaf124 (2025).
60. Rauhut, R. et al. Molecular architecture of the Saccharomyces cerevisiae activated spliceosome. *Science* **353**, 1399–1405 (2016).
61. Bao, P., Will, C. L., Urlaub, H., Boon, K. L. & Lührmann, R. The RES complex is required for efficient transformation of the precatalytic B spliceosome into an activated Bact complex. *Genes Dev.* **31**, 2416–2429 (2017).
62. Galej, W. P., Oubridge, C., Newman, A. J. & Nagai, K. Crystal structure of Prp8 reveals active site cavity of the spliceosome. *Nature* **493**, 638–643 (2013).
63. Umen, J. G. & Guthrie, C. A novel role for a U5 SnRNP protein m 3′ splice site selection. *Genes Dev.* **9**, 855–868 (1995).
64. Mayerle, M. et al. Structural toggle in the RNaseH domain of Prp8 helps balance splicing fidelity and catalytic efficiency. *Proc. Natl. Acad. Sci. USA* **114**, 4739–4744 (2017).
65. Schellenberg, M. J. et al. A conformational switch in PRP8 mediates metal ion coordination that promotes pre-mRNA exon ligation. *Nat. Struct. Mol. Biol.* **20**, 728–734 (2013).
66. Jia, X. & Sun, C. Survey and summary: Structural dynamics of the N-terminal domain and the Switch loop of Prp8 during spliceosome assembly and activation. *Nucleic Acids Res.* **46**, 3833–3840 (2018).
67. Plaschka, C., Lin, P. C., Charenton, C. & Nagai, K. Prespliceosome structure provides insights into spliceosome assembly and regulation. *Nature* **559**, 419–422 (2018).
68. Janke, C. et al. A versatile toolbox for PCR-based tagging of yeast genes: new fluorescent proteins, more markers and promoter substitution cassettes. *Yeast* **21**, 947–962 (2004).
69. Knop, M. et al. Epitope tagging of yeast genes using a PCR-based strategy: more tags and improved practical routines. *Yeast* **15**, 963–972 (1999).
70. Barral, Y., Jentsch, S. & Mann, C. Cyclin Turnover and nutrient uptake are controlled by a common pathway in yeast. *Genes Dev.* **9**, 399–409 (1995).

71. Inada, M. & Pleiss, J. A. Genome-wide approaches to monitor pre-mRNA splicing. *Methods Enzymol.* **470**, 51–75 (2010).
72. Davarinejad, H. Quantifications of Western blots with ImageJ. http://rsb.info.nih.gov/ij/ (2015).
73. Yan, C., Wan, R., Bai, R., Huang, G. & Shi, Y. Structure of a yeast activated spliceosome at 3.5 Å resolution. *Science* **353**, 904–911 (2016).
74. Wan, R., Bai, R., Yan, C., Lei, J. & Shi, Y. Structures of the catalytically activated yeast spliceosome reveal the mechanism of branching. *Cell* **177**, 339–351.e13 (2019).
75. Li, X. et al. CryoEM structure of Saccharomyces cerevisiae U1 snRNP offers insight into alternative splicing. *Nat. Commun.* **8**, 1035 (2017).
76. Nguyen, T. H. D. et al. Cryo-EM structure of the yeast U4/U6.U5 tri-snRNP at 3.7 Å resolution. *Nature* **530**, 298–302 (2016).

Acknowledgements

We thank S. Jentsch for support; C. Guthrie, M. Konarska, K., and M. Rosbash for reagents; and A. Anil and B. Mohapatra for their inputs and technical support. The work in SKM laboratory has been supported by IISER Mohali and the Centre for Protein Science Design and Engineering (CPSDE) of the Ministry of Human Resource and Development (MHRD-14-0064), Government of India; the Max Planck Society, Germany; and the Wellcome Trust/DBT India Alliance Fellowship/Grant [IA/I/18/2/504020 to S.K.M.]. A.K.B. was supported by an ICMR fellowship (JRF-2019/HRD-036) and IISER Mohali.

Author contributions

S.K.M. initiated the study in the Jentsch laboratory at the MPI Biochemistry, Martinsried, Germany. A.K.B., P.C., B.R.P., A.V., and S.K.M. designed and performed the experiments and analysed the data. A.K.B. and S.K.M. collated the data and prepared the manuscript with inputs from other authors.

Competing interests

The authors declare no competing interests.

Additional information

Supplementary information The online version contains supplementary material available at https://doi.org/10.1038/s41467-025-67659-8.

Correspondence and requests for materials should be addressed to Shravan Kumar Mishra.

Peer review information *Nature Communications* thanks the anonymous reviewers for their contribution to the peer review of this work. A peer review file is available.